CHEMISTRY
A EUROPEAN JOURNAL

DOI: 10.1002/chem.201001676

# Low-Temperature Synthesis of Visible-Light Active Fluorine/Sulfur Co-doped Mesoporous $TiO_2$ Microspheres

**Guidong Yang,[a, b] Tiancun Xiao,*[b] Jeremy Sloan,[c] Guoqiang Li,[b] and Zifeng Yan*[a]**

$TiO_2$ nanomaterials with controlled morphologies have attracted extensive interest because of potential applications in solar energy conversion, environmental cleanup and hydrogen generation.[1–3] Nanoscale titanium dioxides have been produced as nanotubes,[3] nanosheets,[4] nanowires[5] and mesoporous microspheres[6] by a variety of approaches. Among the various nanomaterials, mesoporous microspheres have drawn considerable attention due to the intrinsic shape-dependent properties, including high surface area, tuneable pore structure, large pore volume and good surface permeability, in addition to unique optical, electronic, magnetic and catalytic properties.[6] Mesoscale $TiO_2$ spheres can be used in catalysis, separation, ionic intercalation, photonic devices and size-selective reactions.[6] Mesoporous $TiO_2$ micro- and nanostructures are also considered promising candidates for harvesting optical absorption with enhanced energy-conversion efficiency.

There is, however, a drawback that limits more extensive applications of mesoscale $TiO_2$ microspheres; this photo-catalyst exhibits activity predominantly under ultraviolet (i.e., $\lambda < 388$ nm) irradiation, leading to only a narrow utilisation of the visible-light spectrum that accounts for 43% of the total incoming solar energy. A lot of effort has therefore been devoted to modify the band gap of $TiO_2$ by doping to extend the optical absorption properties into the visible spectrum. For example, it was reported that mono-doping of $TiO_2$ with N,[7] F[8] and certain transition metals[9] expands the photo-response of $TiO_2$ into the visible region. However, studies also show that mono-doping alone does not guarantee improved photo-catalytic activity because the partially occupied impurity bands can act as recombination centres and therefore reduce the photo-generated current.[10] More recently, band-gap engineering of $TiO_2$ nanospheres by co-doping with two non-metals has received more attention due to the fact that the defect bands are passivated and hence not effective as carrier recombination centres.[11] However, no related mesoporous $TiO_2$ microspheres co-doped with non-metals have been reported to date.

The ability to control the morphology and chemical composition of the mesoporous microspheres would enable a great light-harvesting capacity and high activity for the synthesised $TiO_2$ photo-catalyst. Herein, we propose a simple and effective method for the fabrication of anatase $TiO_2$ microspheres at a low temperature. The preparation conditions are much milder than those of conventional methods. Meanwhile, a co-doping approach redshifts the threshold of the $TiO_2$ adsorption into the visible-light region and improves the photo-catalytic efficiency for degradation of organic dyes.

The nitrogen adsorption–desorption isotherm and Barrett–Joiner–Halenda (BJH) pore size distribution curves of H-400 and H-600 (calcinated at 400 and 600 °C, respectively) are shown in Figure 1. The adsorption isotherms of both H-400 and H-600 show typical IV isotherms, indicating that the obtained $TiO_2$ microspheres are characteristic for mesoporous material and the adsorption hysteresis loop of the isotherm is close to the type H4 according to the IUPAC classification;[12] this suggests the presence of slit-like pores in the samples. The pore size distribution curves (inset in Figure 1), calculated by the BJH method based on the desorption branch, show that the $TiO_2$ microspheres have a very clear mesoporous structure. As the calcination temperature increases from 400 to 600 °C, the average pore size of

[a] Dr. G. Yang, Prof. Z. Yan
State Key Laboratory of Heavy Oil Processing
China University of Petroleum
Qingdao, 266555 (P.R. China)
Fax: (+86) 532-8698-1295
E-mail: zfyancat@upc.edu.cn

[b] Dr. G. Yang, Dr. T. Xiao, Dr. G. Li
Inorganic Chemistry Laboratory, Department of Chemistry,
University of Oxford, Oxford, OX1 3QR (UK)
Fax: (+44) 1865-272690
E-mail: xiao.tiancun@chem.ox.ac.uk

[c] Dr. J. Sloan
Department of Physics, University of Warwick
Coventry CV4 7AL (UK)

Supporting information for this article is available on the WWW under http://dx.doi.org/10.1002/chem.201001676.

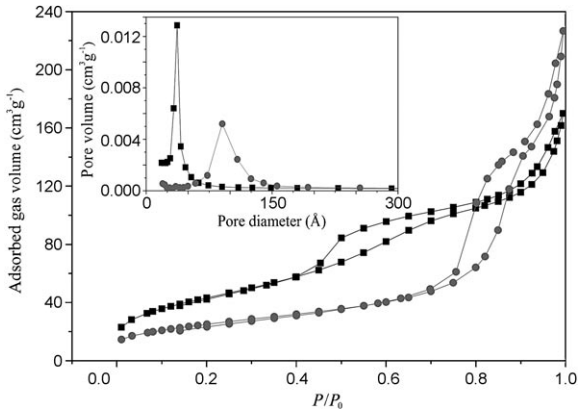


Figure 1. The nitrogen adsorption–desorption isotherm and pore size distribution of H-400 (■) and H-600 (●).

the samples grow from 5.5 to 12.6 nm. This is possibly ascribed to the removal of some residual carbon atoms at high temperatures. As listed in Table S1 in the Supporting Information, the BET surface area of the $TiO_2$ sphere was reduced from 160.0 to 91.6 $m^2g^{-1}$. In contrast, the pore volume increased from 0.27 to 0.35 $cm^3g^{-1}$.

To investigate the phase purity and crystal size of the mesoporous $TiO_2$ sphere, the samples were investigated by XRD analysis and the data are shown in Figure 2. Although

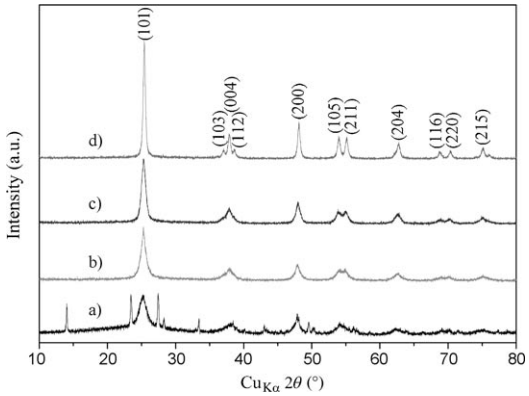


Figure 2. X-ray diffraction patterns of mesoporous $TiO_2$ microspheres annealed at varying temperatures: a) 140, b) 400, c) 500 and d) 600 °C.

the crystallisation temperature of the solvothermal treatment was as low as 140 °C, well-crystallised anatase titanium was observed in the as-prepared microsphere sample (Figure 2a), suggesting that the preparation method is very effective for the synthesis of the $TiO_2$ nanocrystals even at low temperatures. Figure 2b–d show the XRD patterns of the microspheres obtained at various calcination temperatures. All of the diffraction peaks of the mesoporous spheres can be assigned to anatase $TiO_2$ (JCPDS cards 71-1168) and no trace of the rutile phase was detected in the XRD patterns. Based on the Scherrer formula, we can also calculate that the average size of the nanoparticles of these spheres. The H-400, H-500 and H-600 samples were found to possess mean particle sizes of about 20, 24 and 43 nm, respectively. This indicates that the particles that were agglomerated at higher temperatures underwent sintering. The high-resolution (HR) TEM image of H-400 and the TEM image of H-500 obtained at high magnification are provided in Figure S2 in the Supporting Information. Both of the mesoporous $TiO_2$ microspheres were aggregated nanoparticles and the average particle sizes of H-400 and H-500 were around 15–20 and 20–30 nm, respectively. The HRTEM image also confirmed that the $TiO_2$ nanoparticles were mono-crystals.

Figure 3 shows an SEM image of the typical morphology (if not particle or pore size) observed in all of the preparations. Some porosity is evident in the particles as a result of

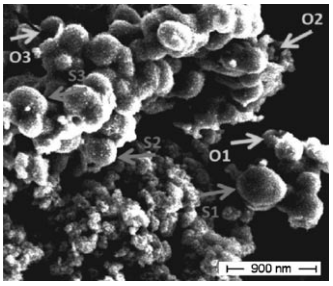


Figure 3. SEM image of H-500 with aggregated particle sizes in the range 400–500 nm. Some particles (i.e., S1–S3) are closed, whereas others are more cup-like (i.e., O1–O3). Scale bar = 900 nm.

the a cup-like appearance of some, whereas others are sealed similar to preparations produced by Chen et al. and Wang et al.[13] As shown in Figure S3 in the Supporting Information, the TEM image of H-500 also reveals that the as-prepared mesoporous $TiO_2$ microsphere is composed of a hollow structure and solid spherical particles.

Figure 4 shows TEM images of $TiO_2$ microspheres obtained at two different calcination temperatures. Both catalysts have representative microsphere structures. The H-600 sample (Figure 4a) shows larger spherical particles, with an average diameter of 300–400 nm, than the H-400 sample (100–200 nm in diameter, Figure 4c). The EDX analysis shows that the mesoporous microsphere is composed of Ti, O and S. Fluorine was not observed in these spectra, probably due to the overlap between F and O at the same energy position. The SAED analysis further confirmed that the product is composed of poly-crystalline aggregates of an anatase nanostructure, consistent with the X-ray diffraction findings.

On the basis of all of the observations, we can propose a possible formation mechanism for the synthesis of the mesoporous $TiO_2$ microsphere; this is represented schematically in Figure 5. Glacial acetic acid plays a vital role in the preparation of the mesoporous particles because it can stabilise and restrict the hydrolysis process of $Ti(OBu)_4$ and lead to the generation of the $[Ti(OBu)_{4-n}(CH_3COO)_n]$ precursor. In addition, glucose molecules can self-assemble by hydrogen

  

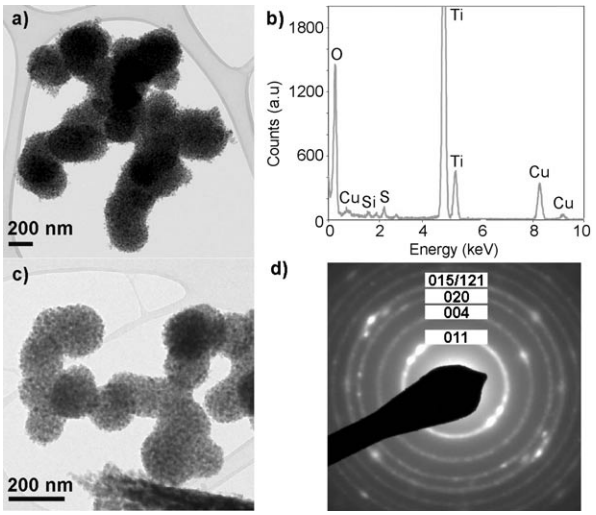


Figure 4. a) TEM image of H-600 and b) corresponding energy-dispersive X-ray (EDX) pattern. c) TEM image of H-400 and d) corresponding selected-area electron diffraction (SAED).

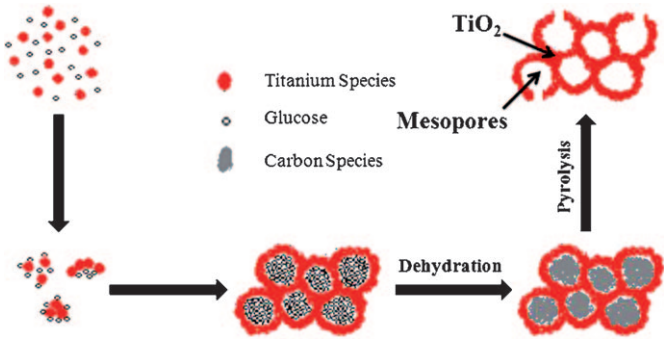


Figure 5. Illustration of the suggested formation mechanisms of mesoporous $TiO_2$ microspheres during the solvothermal process.

bonding to generate round globules under acidic conditions. Therefore, in the initial stages, the small amorphous [Ti-$(OBu)_{4-n}(CH_3COO)_n$] nanoparticles (Ti species) form quickly and then the [$Ti(OBu)_{4-n}(CH_3COO)_n$(acid)(glucose)] particles are formed by weak coordination interactions and hydrogen bonding. During the solvothermal reaction, glucose spontaneously aggregates into large spheres to minimise the free energy of the system, while the high temperature drives the [$Ti(OBu)_{4-n}(CH_3COO)_n$(acid)(glucose)] species to react with oxygen and instantly self-assemble to yield an incompact $TiO_2$ nanoparticle layer on the exterior of the glucose globules. As the reaction proceeds, the dehydration of glucose occurs and then transformation of glucose to carbonaceous polysaccharide globules (carbon species). The remaining carbonaceous cores can be easily removed under the calcination process, eventually resulting in the formation of mesoporous $TiO_2$ spheres.

The X-ray photoelectron spectroscopy (XPS) studies of H-400 (see Figure S4 in the Supporting Information) show that the mesoporous $TiO_2$ microsphere contains the elements Ti, O, F, S and C; this is in accordance with our previous study.[15] The atomic concentrations of the F and S in the H-400 sample were found to be 2.92 and 3.33 at.%, respectively. Although nitrogen was introduced into the synthetic system through $NH_4F$, none was detected by either XPS or EDX in the H-400 sample, indicating that nitrogen is not doped into the $TiO_2$ lattice by the current preparation method.

To test the activity of the microspheres, we chose methyl orange (MO) as a target to evaluate the photo-catalytic behaviour of the microspheres. MO is very stable and does not normally degrade under visible or ultraviolet light, except when assisted by an appropriate photo-catalyst. A xenon lamp, equipped with a 420 nm cut-off filter to completely remove the UV light and ensure illumination by visible light only, was therefore used as the light source.

Figure 6 shows the visible-light-induced photo-catalytic decomposition of the MO solution by the mesoporous $TiO_2$ microspheres. Un-doped $TiO_2$ microspheres show no activity

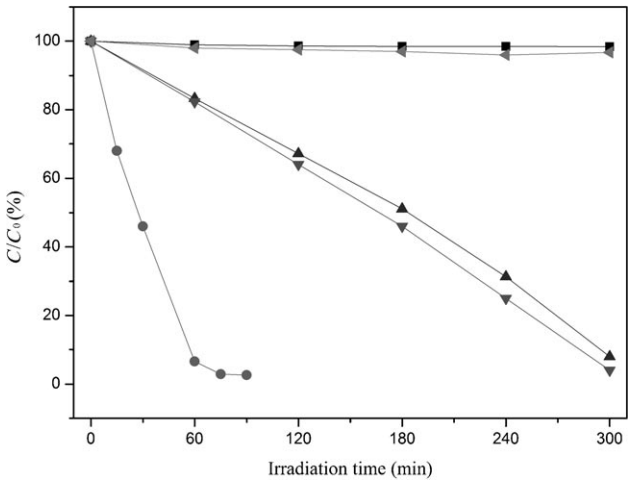


Figure 6. Photo-catalytic degradation of MO by different mesoporous $TiO_2$ microspheres under visible-light irradiation ($\lambda > 420$ nm). ■: no catalyst, ●: H-400, ▲: H-500, ▼: H-600 and ◀: un-doped $TiO_2$.

due to the big energy gap (3.2 eV, the activity of commercial P25 $TiO_2$ is not shown because the properties and the synthetic method are quite different to our samples), whereas all of the mesoporous sphere samples exhibit high photocatalytic activity under visible-light irradiation, owing to the F and S co-doping promoting formation of S–O–Ti and F–Ti bonds (see Figure S4 and S5 in the Supporting Information). The S doping may possibly generate an intermediate energy level above the valence band of $TiO_2$ and thereby narrowing the band gap to induce visible-light absorption. The fluorine dopant theoretically does not contribute to the observed visible-light absorption of $TiO_2$ spheres due to the fact that the F 2p localised level appears below the bottom of the O 2p valence band of $TiO_2$. These F impurity states do not mix with either the valence band or the conduction

  

band of $TiO_2$, which has already been confirmed by theoretical band calculations.[14] However, F doping can promote the creation of oxygen vacancies in the bulk or over the surface of $TiO_2$ and in this way induce a magnetic resonance detected by EPR experiments (see Figure S6 in the Supporting Information). The contributions of these oxygen vacancies not only cause the optical absorption of mesoporous structure $TiO_2$ in the visible-light region, but also act as active sites to produce oxidising species enhancing the photo-catalytic activity.[15] The H-500 and H-600 samples therefore have a clear visible-light activity. Among the three samples, H-400 exhibit much greater activity than the photo-catalysts annealed above 400 °C, indicating that the calcination temperature has a significant influence on the photo-catalytic behaviour of the $TiO_2$ microspheres. A higher annealing temperature (> 400 °C) would induce crystal growth and a greater particle size. Smaller particle sizes of $TiO_2$ provide greater surface area to volume ratios and thus induce better photocatalytic activity, and more importantly, the H-400 sample shows stronger visible-light absorption (see Figure S7 in the Supporting Information). Additionally, it is believed that synergistic effects between F and S dopants co-doped into the $TiO_2$ lattice leads to the enhancement of sunlight photoactivities. In addition to higher activity, the H-400 sample also shows stronger durability in the successive photo-reaction process. After six cycles, the photo-degradation yield of MO still reached 91 % in 60 min (see Figure S8 in the Supporting Information).

In summary, the F and S co-doped mesoporous $TiO_2$ microspheres have been successfully fabricated through a simple template solvothermal methodology. The formation of Ti−F and Ti−O−S bonds leads to enhanced visible-light absorption of the $TiO_2$ microsphere. The obtained materials show higher photo-activity for degradation of MO under visible-light irradiation, owing to the synergetic effect of the high surface area, larger pore volume, the well-crystallised anatase structure and stronger visible-light absorption.

## Experimental Section

**Preparation**: In a typical procedure, $NH_4F$ (0.015 mol), $CH_4N_2S$ (0.015 mol), acetic acid (5 mL) and $Ti(OBu)_4$ (0.01 mol) were dispersed in ethanol (60 mL) to form solution A. Meanwhile, glucose (5.4 g) was dissolved in $H_2O$ (6 mL) at 40 °C to form solution B. The two solutions were then mixed for 30 min and heated in an autoclave at 140 °C for 24 h. After cooling to room temperature, the $TiO_2$ microsphere (see Figure S1 in the Supporting Information) was collected by centrifugation, washed with deionised water and then dried at 80 °C overnight prior to annealing at 400, 500 or 600 °C for 3 h. The as-prepared samples were denoted as H-400, H-500 and H-600, respectively.

**Characterisation**: Nitrogen adsorption–desorption isotherms were measured at 77 K by an ASAP3000 adsorption apparatus from Micromeritics. The samples were degassed at 100 °C overnight under vacuum before analysis. The crystal size and crystalline structure of the $TiO_2$ samples were determined by XRD with a Philips X-PeRT Pro Alpha 1 diffractometer operating with $Cu_{K\alpha}$ radiation ($\lambda = 1.5406$ Å) at a tube current of 40 mA and a voltage of 45 kV. The geometry and morphology of the $TiO_2$ particles were observed with JEOL 2000FX (TEM) and JSM840F instruments (SEM).A JEOL JEM-3000F microscope (HRTEM) was used to characterise the nanostructures. Fourier-transform infrared (FTIR) spectra were obtained with a Bruker Vertex-70 by the diffused-reflectance-accessory technique. UV/Vis diffuse reflectance was recorded by a Perkin–Elmer Lambda 750S UV/Vis spectrometer. The EPR spectra were recorded on an X-band Bruker EMX spectrometer. XPS was performed with a Perkin–Elmer RBD upgraded PHI-5000C ESCA system with mono-chromatic $Mg_{K\alpha}$ excitation. All bonding energies were calibrated to the C 1s internal standard peak (284.8 eV) of surface carbon atoms.

**Photo-catalytic activity testing**: The photo-catalytic testing of the degradation of MO was carried out in a self-designed 200 mL reactor with a cooling-water-cycle system keeping the reaction temperature constant. A xenon lamp (Trusttech, Beijing, China) was used as the visible-light source. UV light of wavelengths shorter than 420 nm was removed by a glass filter. The distance between the strip lamp and the fluid level was kept as 15 cm. The initial concentration of the MO solution was 10 mg $L^{-1}$. The $TiO_2$ catalyst (80 mg) and the MO aqueous solution (100 mL) were added into the reaction system. Before the light was switched on, the suspension was kept under magnetic stirring for 150 min to make sure the mixture reached the adsorption equilibrium (see Figure S9 in the Supporting Information). And then the photo-catalytic reaction was performed under visible-light illumination. During the photo-reactions process, 3 mL of the solution was taken out with a constant frequency and the photo-catalyst was separated from the solution by centrifugation. The concentration of the remaining clear liquid was tested by a UV/Vis spectrometer. No oxygen was bubbled into the suspension during the photo-reaction.

## Acknowledgements

We thank the UK Photo-catalysis Network for their kind support. G. Y. acknowledges a scholarship from the China Scholarship Council (CSC).

**Keywords:** doping · mesoporous materials · microspheres · titanium · visible light

[1] D. P. Serrano, G. Calleja, R. Sanz, P. Pizarro, *Chem. Commun.* **2004**, 1000.
[2] O. Carp, C. L. Huisman, A. Reller, *Prog. Solid State Chem.* **2004**, *32*, 33.
[3] Z. Jiang, F. Yang, N. Luo, B. T. T. Chu, D. Sun, H. Shi, T. Xiao, P. P. Edwards, *Chem. Commun.* **2008**, 6372.
[4] H. G. Yang, G. Liu, S. Z. Qiao, C. H. Sun, Y. G. Jin, S. C. Smith, J. Zou, H. M. Cheng, G. Q. Lu, *J. Am. Chem. Soc.* **2009**, *131*, 4078.
[5] Y. J. Hwang, A. Boukai, P. Yang, *Nano Lett.* **2009**, *9*, 410.
[6] a) Y. Zhang, G. Li, Y. Wu, Y. Luo, L. Zhang, *J. Phys. Chem. B* **2005**, *109*, 5478; b) L.-S. Zhong, J.-S. Hu, L.-J. Wan, W.-G. Song, *Chem. Commun.* **2008**, 1184; c) A. Corma, *Chem. Rev.* **1997**, *97*, 2373; d) A. S. Aricò, P. Bruce, B. Scrosati, J. M. Tarascon, W. Van Schalkwijk, *Nat. Mater.* **2005**, *4*, 366; e) Y. K. Hwang, K.-C. Lee, Y.-U. Kwon, *Chem. Commun.* **2001**, 1738.
[7] a) X. Chen, X. Wang, Y. Hou, J. Huang, L. Wu, X. Fu, *J. Catal.* **2008**, *255*, 59; b) G. Yang, Z. Jiang, H. Shi, T. Xiao, Z. Yan, *J. Mater. Chem.* **2010**, *20*, 5301; c) S.-K. Joung, T. Amemiya, M. Murabayashi, K. Itoh, *Chem. Eur. J.* **2006**, *12*, 5526.
[8] a) W. Ho, J. C. Yu, S. Lee, *Chem. Commun.* **2006**, 1115; b) J. Tang, H. Quan, J. Ye, *Chem. Mater.* **2007**, *19*, 116.
[9] X. Yan, J. He, D. G. Evans, X. Duan, Y. Zhu, *Appl. Catal. B* **2005**, *55*, 243.
[10] T. Umebayashi, T. Yamaki, H. Itoh, K. Asai, *J. Phys. Chem. Solids* **2002**, *63*, 1909.

  

[11] a) K-S. Ahn, Y. Yan, S. Shet, T. Deutsch, J. Turner, M. Al-Jassim, *Appl. Phys. Lett.* **2007**, *91*, 231909; b) Y. Gai, J. Li, S.-S. Li, J.-B. Xia, S.-H. Wei, *Phys. Rev. Lett.* **2009**, *102*, 036402.
[12] K. S. W. Sing, D. H. Everett, R. A. W. Haul, L. Moscou, R. A. Pierotti, J. Rouquerol, T. Siemieniewska, *Pure Appl. Chem.* **1985**, *57*, 603.
[13] a) T. Chen, P. J. Colver, S. A. F. Bon, *Adv. Mater.* **2007**, *19*, 2286; b) H. Wang, Z. Wu, Y. Liu, *J. Phys. Chem. C* **2009**, *113*, 13317.
[14] a) K. Mori, K. Maki, S. Kawasaki, S. Yuan, H. Yamashita, *Chem. Eng. Sci.* **2008**, *63*, 5066; b) J. C. Yu, J. Yu, W. Ho, Z. Jiang, L. Zhang, *Chem. Mater.* **2002**, *14*, 3808; c) J. K. Zhou, L. Lv, J. Yu, H. L. Li, P. Z. Guo, H. Sun, X. S. Zhao, *J. Phys. Chem. C* **2008**, *112*, 5316.
[15] a) G. Yang, Z. Jiang, H. Shi, M. O. Jones, T. Xiao, P. P. Edwards, Z. Yan, *Appl. Catal., B* **2010**, *96*, 458.

Received: June 13, 2010
Published online: December 16, 2010

  